

Simulation of pattern dynamics of cohesive granular particles under a plane shear

Satoshi Takada and Hisao Hayakawa

Yukawa Institute for Theoretical Physics, Kyoto University, Kitashirakawa Oiwakecho, Sakyo-ku, Kyoto 606-8502 Japan

Abstract. We have performed three-dimensional molecular dynamics simulation of cohesive granular particles under a plane shear. From the simulation, we found the existence of three distinct phases in steady states: (I) a uniform shear phase, (II) a coexistent phase of a shear band and a gas region and (III) a crystal phase. We also found that the critical line between (II) and (III) is approximately represented by $\zeta \propto \exp(\beta\dot{\gamma}L_y)$, where ζ , β , $\dot{\gamma}$, L_y are the dissipation rate, an unimportant constant, the shear rate and the system size of the velocity gradient direction, respectively.

Keywords: granular physics, pattern formation, molecular dynamics simulation

PACS: 45.70.Qj, 47.11.Mn, 64.60.Ht

INTRODUCTION

The interactions among macroscopic granular particles, such as sands, are characterized by a repulsive and a dissipative ones. The energy dissipation through inelastic collisions causes destabilization of a uniform state of the system. It is known that there appear clusters in such systems [1, 2], which may be understood by the hydrodynamic equations [3, 4, 5, 6]. When a shear is applied to the granular system, high-density region, called "shear band", appears [7]. There exist many papers to estimate the transport coefficients by using kinetic theory [8, 9, 10, 11, 12, 13] and to analyze the pattern dynamics by using continuum mechanics [14, 15, 16, 17, 18, 19, 20, 21, 22].

On the other hand, fine powders of submicron order, such as tonner particles or interstellar dusts, have attractive forces such as an electrostatic force [23]. The existence of the attractive force causes some new features due to the competition of the gas-liquid phase transition [24, 25, 26] and the dissipative structure [7]. For instance, nucleation process near equilibrium is well understood [27], but that under a shear is not well understood. In this paper, we try to characterize the non-equilibrium pattern formation of fine powders under a plane shear based on the three dimensional molecular dynamics simulation.

MODEL AND SETUP

The system we consider consists of monodisperse $N(= 10,000)$ spheres, whose radius is σ and mass is m . The system size is $L_x \times L_y \times L_z$ ($L \equiv L_x = L_y$) and we choose x -axis as the shear direction and y -axis as the ve-

locity gradient direction. We assume that the interaction between particles is described by the truncated Lennard-Jones potential

$$U^{\text{LJ}}(r_{ij}) = \begin{cases} 4\epsilon \left(\left(\frac{\sigma}{r_{ij}} \right)^{12} - \left(\frac{\sigma}{r_{ij}} \right)^6 \right) & (r \leq r_c) \\ 0 & (\text{else}) \end{cases}, \quad (1)$$

with the well depth ϵ , where $r_{ij} = |\mathbf{r}_{ij}|$ is the distance between i -th and j -th particles and r_c is cut-off length (in this study we use $r_c = 3\sigma$). For the dissipative force, we use

$$\mathbf{F}^{\text{vis}}(\mathbf{r}_{ij}, \mathbf{v}_{ij}) = -\zeta \Theta(\sigma - |\mathbf{r}_{ij}|) (\mathbf{v}_{ij} \cdot \hat{\mathbf{r}}_{ij}) \hat{\mathbf{r}}_{ij}, \quad (2)$$

with the dissipation rate ζ , where \mathbf{v}_{ij} is the relative velocity vector of i -th and j -th particles, $\Theta(r)$ is the step function which is 1 for $r > 0$ and 0 for otherwise, and $\hat{\mathbf{r}}$ is a unit vector proportional to \mathbf{r} . We note that ζ is a dissipation parameter related to the coefficient of restitution e , for example, $e = 0.998$ for $\zeta = 0.1$ and $e = 0.983$ for $\zeta = 1.0$ at the temperature $T = 1.4\epsilon$. Thus, we are interested in weakly dissipative situations. This weak dissipation is necessary to reach a steady state.

In general, the boundary effect is important for granular systems. It is known that the results strongly depend on the boundary condition [28, 29, 30, 31, 32]. In this paper, we adopt Lees-Edwards condition [33, 34] to suppress the boundary effect with the aid of SLLOD algorithm [34, 35]:

$$\frac{d\mathbf{r}_i}{dt} = \frac{\mathbf{p}_i}{m} + \dot{\gamma}y_i\hat{\mathbf{e}}_x, \quad (3)$$

$$\frac{d\mathbf{p}_i}{dt} = \mathbf{F}_i - \dot{\gamma}p_{yi}\hat{\mathbf{e}}_x. \quad (4)$$

This model is known as that the system is relaxed to the uniform shear state near equilibrium, where $\mathbf{r}_i =$

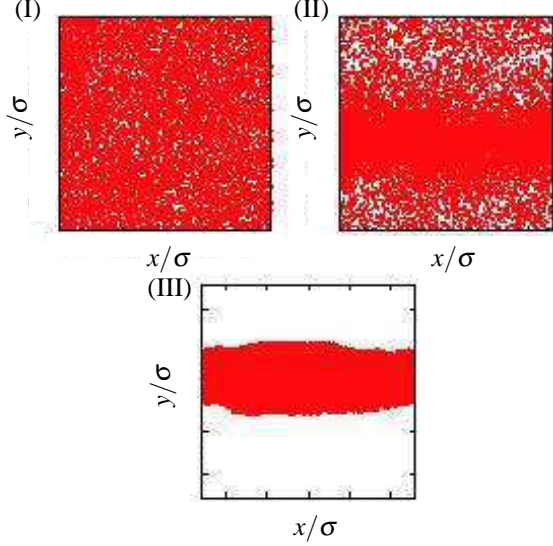


FIGURE 1. Three typical patterns corresponding to three phases in steady states for $\bar{\rho} = 0.308$: (I) uniform shear phase ($\dot{\gamma}^* = 0.88, \zeta^* = 1.0$), (II) coexistent phase of shear band and gas ($\dot{\gamma}^* = 0.66, \zeta^* = 1.0$), and (III) crystal phase ($\dot{\gamma}^* = 0.355, \zeta^* = 1.0$).

$(x_i, y_i, z_i), \mathbf{p}_i = (p_{xi}, p_{yi}, p_{zi})$ are respectively the position and the momentum of i -th ($1 \leq i \leq N$) particle, $\mathbf{v}_i = \dot{\mathbf{r}}_i$, $\dot{\gamma}$ is the shear rate and $\hat{\mathbf{e}}_x$ is the unit vector in x direction. The force acting on i -th particle is given by

$$\mathbf{F}_i = - \sum_{j \neq i} \nabla_i U^{\text{LJ}}(r_{ij}) + \sum_{j \neq i} \mathbf{F}^{\text{vis}}(\mathbf{r}_{ij}, \mathbf{v}_{ij}). \quad (5)$$

In this paper, we choose $T_0 = 1.4\varepsilon$ as the initial temperature, which is slightly higher than the critical temperature for the equilibrium Lennard-Jones fluid [24, 25]. The system is equilibrated in the absence of the shear and the dissipation for $t = 200(m\sigma^2/\varepsilon)^{1/2}$. Then we apply the shear and the dissipation to the system.

RESULTS

At first, we choose the average density $\bar{\rho} = 0.308$, where $\bar{\rho}$ is defined by $N\sigma^3/L^2L_z$. Note that this density corresponds to the critical density for Lennard-Jones fluid at equilibrium [24, 25, 26]. We fix the system size $L_x = L_y = 52\sigma, L_z = 12\sigma$ for this density. We study how the steady state depends on parameters such as the density, the shear rate and the dissipation rate. We found that there exist three distinct steady phases. The typical patterns for these phases are drawn in Fig. 1, where $\dot{\gamma}^* = \dot{\gamma}(m\sigma^2/\varepsilon)^{1/2}$ and $\zeta^* = \zeta(m\sigma^2/\varepsilon)^{1/2}$. The uniform shear phase (I) can be observed for a larger shear rate, and the crystal phase (III) is obtained for smaller shear rate. We found that the coexistence phase (II) between a shear band and the gas region disappears when the shear

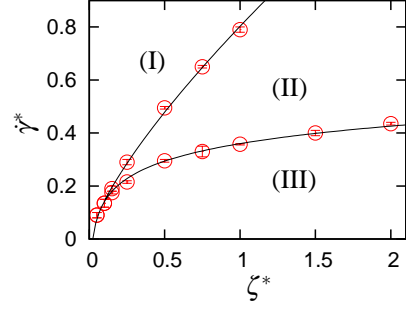


FIGURE 2. The phase boundary lines in the plane of the shear rate $\dot{\gamma}$ and the dissipation rate ζ for the density $\bar{\rho} = 0.308$.

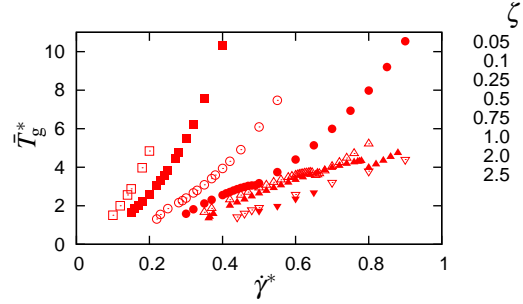


FIGURE 3. The dependence of the average granular temperature \bar{T}_g on the shear rate $\dot{\gamma}$ for several dissipation rates ζ (for $\bar{\rho} = 0.308$).

rate $\dot{\gamma}$ and the dissipative rate ζ become small. The phase boundary lines for $\bar{\rho} = 0.308$ are plotted in Fig. 2.

Now let us reproduce the boundary lines between two phases. For this purpose, we try to characterize the behavior in terms of a simple physical argument based on the granular temperature $T_g \equiv (m/3N) \sum_{i=1}^N |\mathbf{v}_i - \bar{\mathbf{v}}|^2$ [36, 37], where $\bar{\mathbf{v}} = \bar{\mathbf{v}}(y, t)$ is the velocity field of the y -axis. We measure the time averaged granular temperature \bar{T}_g , changing the shear rate $\dot{\gamma}$.

The dependence of \bar{T}_g on the shear rate $\dot{\gamma}$ for several dissipation rates ζ is showed in Fig. 3, where $\bar{T}_g^* = \bar{T}_g/\varepsilon$. In the case of the phase (I), the granular temperature satisfies $\bar{T}_g \propto \dot{\gamma}^2$, which is consistent with the results of dimensional analysis [37, 38]. On the contrary, the granular temperature T_g becomes zero as time goes on, i.e. $\bar{T}_g = 0$ in the phase (III).

Here, we investigate the dependence of \bar{T}_g on $\dot{\gamma}$ in the phase (II). A typical configuration of the particles is presented in Fig. 4. We can separate the system into two regions: (i) the shear band region, and (ii) the gas region.

To this end, we consider the density profile $\rho(y)$, which is defined as follows: we count the number of particles in the region $(j-1)\sigma < y < j\sigma$, where j is an integer, and calculate the local average density ρ_j in that region. If $\rho_j > \bar{\rho}$, this region is regarded as a part of (i), otherwise the region is (ii). We introduce n_{sb} and T_{sb} as

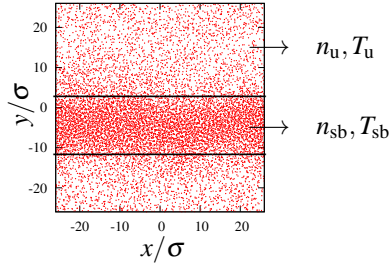


FIGURE 4. Typical configuration in pattern (II) ($\bar{\rho} = 0.308, \dot{\gamma}^* = 0.66, \zeta^* = 1.0$). The system is separated into two regions as a function of the local density $\rho(y)$ and the average density $\bar{\rho}$: (i) the shear band region, and (ii) the gas region.

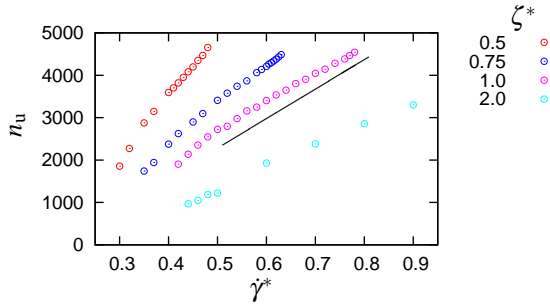


FIGURE 5. The number of particles in the region (ii) n_u vs. the shear rate $\dot{\gamma}$.

the number and the granular temperature in the region (i) respectively. n_u and T_u are the corresponding ones in the region (ii). The average granular temperature of the system \bar{T}_g is given by

$$\bar{T}_g = \frac{N - n_u}{N} T_{sb} + \frac{n_u}{N} T_u. \quad (6)$$

For $\bar{\rho} = 0.308$, the relationship between the shear rate $\dot{\gamma}$ and the number of particles in region (ii) n_u is plotted in Fig. 5. From Fig. 5, we approximately found $n_u \propto \dot{\gamma}$. The relationships between $\dot{\gamma}$ and T_u and between $\dot{\gamma}$ and T_{sb} are plotted in Fig. 6, where we approximately found $T_u \simeq const.$, $T_{sb} \propto \dot{\gamma}$. From Eq. (6), we may write the

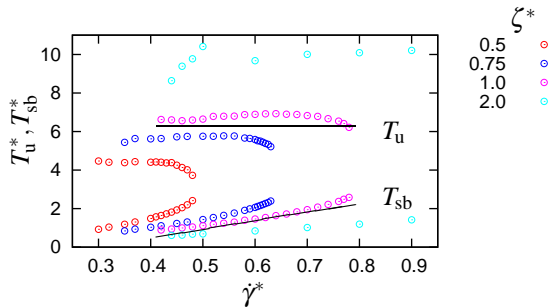


FIGURE 6. The shear rate $\dot{\gamma}$ vs. the granular temperature T_{sb} in the region (i) and T_u in the region (ii).

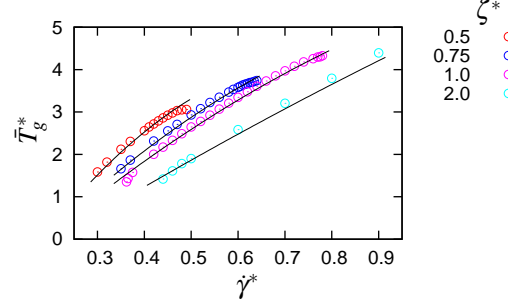


FIGURE 7. The dependence of the average granular temperature T_g on the shear rate $\dot{\gamma}$ for several dissipation rate ζ (open circles) and the results calculated by using Eq. (7) (solid lines).

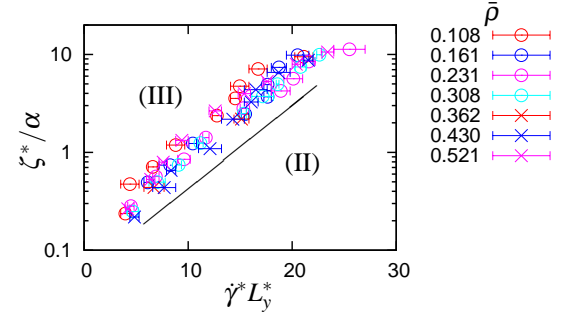


FIGURE 8. Boundary between (II) and (III) for each density $\bar{\rho}$, where the solid line indicates $\zeta \propto \alpha \exp(\beta \dot{\gamma} L_y)$ with the density dependent α .

relation

$$\begin{aligned} \bar{T}_g^* &= \frac{N - n_u}{N} T_{sb}^* + \frac{n_u}{N} T_u^* \\ &= a \dot{\gamma}^* - b \dot{\gamma}^{*2} + c, \end{aligned} \quad (7)$$

where $\bar{T}_g^* = \bar{T}_g/\varepsilon$, $T_{sb}^* = T_{sb}/\varepsilon$ and $T_u^* = T_u/\varepsilon$. Here a, b, c are constants with respect to the shear rate while they depend on the density and the dissipation rate.

The dependence of \bar{T}_g on the shear rate $\dot{\gamma}$ calculated from the definition and that from Eq. (7) are plotted in Fig. 7. We found that the expression (7) well reproduces the results of our simulation.

Now let us study the dependence of the phase boundary lines among the phases on the density. For this purpose, we investigate the behavior of $\bar{\rho} = 0.108, 0.161, 0.231, 0.308, 0.362, 0.430, 0.521$ ($L_y = 88\sigma, 72\sigma, 60\sigma, 48\sigma, 44\sigma, 40\sigma$) in the plane of the shear rate $\dot{\gamma}$ and the dissipation rate ζ for several $\bar{\rho}$. From our simulation, we found that the phase boundary between (II) and (III) is describes by

$$\zeta^* = \alpha \exp(\beta \dot{\gamma}^* L_y^*), \quad (8)$$

where $L_y^* = L_y/\sigma$. Here, α and β are constants with respect to the shear rate and the dissipation rate, but α

solely depends on the density $\alpha = \alpha(\rho)$ as

$$\alpha(\rho) = 453.66\rho^5 - 721.97\rho^4 + 425.66\rho^3 - 114.02\rho^2 + 13.62\rho - 0.3746. \quad (9)$$

Note that β is independent of the density. The physical reason of Eq. (8) can be understood as follows. The boundary between phase (II) and phase (III) might be determined by the condition whether the particle trapped in the potential can pop out. The energy gained by a shear δE is proportional to $\dot{\gamma}^2 L_y^2$, and the granular temperature T_{sb} in the shear band is proportional to $\dot{\gamma} L_y$ (the inverse temperature is proportional to $(\dot{\gamma} L_y)^{-1}$). From these relations, the probability of pop out p satisfies the relation $p \propto e^{-\beta \dot{\gamma} L_y}$, which means $1/\tau \sim \zeta t^* e^{-\beta \dot{\gamma} L_y}$, where τ is characteristic time scale of pop out and $(\zeta t^*)^{-1}$ is that of the dissipation. Therefore this relation becomes $\zeta \propto \exp(\beta \dot{\gamma} L_y)$.

CONCLUSION

We have clarified the relations between the shear rate and the dissipation rate in the system for cohesive particles under a plane shear. In the phase (II), we found that the dependence of the granular temperature on the shear rate is approximately given by $T_g = a\dot{\gamma} - b\dot{\gamma}^2 + c$. We also found that the boundary between (II) and (III) is approximately described by $\zeta \propto \exp(\beta \dot{\gamma} L_y)$.

We suppose that the mechanism of the boundary between (I) and (II) is related to the stability criterion for granular gas [14, 15, 16, 17, 18, 19, 20, 21, 22]. This will be a future subject of our study.

ACKNOWLEDGMENTS

Numerical computation in this work was carried out at the Yukawa Institute Computer Facility. This work is partially supported by and the Grant-in-Aid for the Global COE program AgThe Next Generation of Physics, Spun from Universality and Emergence from MEXT, Japan.

REFERENCES

1. I. Goldhirsch, and G. Zanetti, *Phys. Rev. Lett.* **70**, 1619–1622 (1993).
2. I. Goldhirsch, M.-L. Tan, and G. Zanetti, *J. Sci. Comput.* **8**, 1–40 (1993).
3. S. McNamara, *Phys. Fluid A* **5**, 3056–3070 (1993).
4. S. McNamara, and W. R. Young, *Phys. Rev. E* **53**, 5089–5100 (1996).
5. N. Brilliantov, C. Salueña, T. Schwager, and T. Pöschel, *Phys. Rev. Lett.* **93**, 134301-1–4 (2004).
6. N. V. Brilliantov, and T. Pöschel, *Kinetic Theory of Granular Gases*, Oxford University Press, Oxford, 2004, pp. 223–251.
7. K. Saitoh, and H. Hayakawa, *Phys. Rev. E* **75**, 021302-1–11 (2007).
8. J. T. Jenkins, and S. B. Savage, *J. Fluid Mech.* **130**, 187–202 (1983).
9. J. F. Lutsko, *Phys. Rev. E* **72**, 021306-1–23 (2005).
10. V. Garzó, and J. W. Dufty, *Phys. Rev. E* **59**, 5895–5911 (1999).
11. C. K. K. Lun, S. B. Savage, D. J. Jeffrey, and N. Chepurny, *J. Fluid Mech.* **140**, 223–256 (1984).
12. N. Sela, I. Goldhirsch, and S. H. Noskovicz, *Phys. Fluids* **8**, 2337–2353 (1996).
13. J. M. Montanero, V. Garzó, A. Santos, and J. J. Brey, *J. Fluid Mech.* **389**, 391–411 (1999).
14. K. Saitoh, and H. Hayakawa, *Granul. Matter* **13**, 697–711 (2011).
15. M. Alam, *Prog. Theor. Phys. Supp.* **195**, 78–100 (2012).
16. M. Alam, and P. R. Nott, *J. Fluid Mech.* **377**, 99–136 (1998).
17. M. Alam, and P. R. Nott, *J. Fluid Mech.* **343**, 267–301 (1997).
18. S. B. Savage, *J. Fluid Mech.* **241**, 109–123 (1992).
19. V. Garzó, *Phys. Rev. E* **73**, 021304-1–19 (2006).
20. P. J. Schmid, and H. K. Kytömaa, *J. Fluid Mech.* **264**, 255–275 (1994).
21. B. Gayen, and M. Alam, *J. Fluid Mech.* **567**, 195–233 (2006).
22. P. R. Nott, M. Alam, K. Agrawal, R. Jackson, and S. Sundaresan, *J. Fluid Mech.* **397**, 203–229 (1999).
23. A. Castellanos, *Adv. Phys.* **54**, 263–376 (2005).
24. J.-P. Hansen, and L. Verlet, *Phys. Rev.* **184**, 151–161 (1969).
25. B. Smit, *J. Chem. Phys.* **96**, 8639–8640 (1992).
26. H. Watanabe, N. Ito, and C.-K. Hu, *J. Chem. Phys.* **136**, 204102-1–7 (2012).
27. K. Yasuoka, and M. Matsumoto, *J. Chem. Phys.* **109**, 8451–8462 (1998).
28. A. Karison, and M. L. Hunt, *J. Heat Transf.* **121**, 984–991 (1999).
29. M. W. Richman, and C. S. Chou, *Z. Angew. Math. Phys.* **39**, 885–901 (1988).
30. R. N. Dave, A. D. Rosato, and K. Bhaswan, *Mech. Res. Commun.* **22**, 335–342 (1995).
31. C. S. Campbell, *J. Fluid Mech.* **348**, 85–101 (1997).
32. M.-L. Tan, and I. Goldhirsch, *Phys. Fluids* **9**, 856–869 (1997).
33. A. W. Lees, and S. F. Edwards, *J. Phys. C: Solid State Phys.* **5**, 1921–1929 (1972).
34. D. J. Evans, and G. P. Morriss, *Statistical Mechanics of Nonequilibrium Liquids Second Edition*, Cambridge University Press, Cambridge, 2008, pp. 130–142.
35. D. J. Evans, and G. P. Morriss, *Phys. Rev. A* **30**, 1528–1530 (1984).
36. I. Goldhirsch, *Powder Technol.* **182**, 130–136 (2008).
37. I. Goldhirsch, *Annu. Rev. Fluid Mech.* **35**, 267–293 (2003).
38. P. K. Haff, *J. Fluid Mech.* **134**, 401–430 (1983).